

Article

Method for the Construction of Urban Road Digital Elevation Models Integrated with Semantic Information

Mingwei Zhao¹ and Na Zhao^{2,3,*} ¹ Geographic Information and Tourism College, Chuzhou University, Chuzhou 239000, China² State Key Laboratory of Resources and Environmental Information System, Institute of Geographic Sciences and Natural Resources Research, Chinese Academy of Sciences, Beijing 100101, China³ College of Resources and Environment, University of Chinese Academy of Sciences, Beijing 100101, China

* Correspondence: zhaon@reis.ac.cn

Abstract: Roads are a type of typical artificial terrain, and are key components of urban terrain. Road networks formed by connections between different roads not only form the skeleton of urban terrain, but also plays an important role in transmitting energy and matter on the urban surface. Therefore, how to consider characteristics when constructing the digital road elevation model (DEM) has become an important research topic in the field of geographic information and mapping. Using high-definition unmanned aerial vehicle (UAV) images as the basic data source, this study proposes a new method for constructing the road DEM by analyzing semantic features such as road shape and function. This method first takes the sideline and centerline of the road as the macroscopic undulation morphological constraints. It uses the shape control equation of the local domain to constrain the morphological change characteristics of the road surface in the transverse and longitudinal directions, in order to construct the road DEM with high fidelity to the surface shape characteristics. Then, in terms of the water catchment function of the road surface, a road DEM correction method considering surface flow direction characteristics is designed to ensure that the water catchment path of the road surface conforms to the actual situation. For this paper, several typical roads in Chuzhou University in Anhui Province, China, were selected as the experimental objects to carry out a DEM construction experiment. The results indicate the following: (1) compared with the traditional construction method, the DEM shape of the road constructed by this research method is more consistent with the actual road shape, and the smoothness of the road surface is better; (2) due to the high density and high elevation accuracy of the point cloud used in modeling, the elevation adjustment strategy of the sideline and centerline of the road implemented in this study does not reduce elevation accuracy, indicating that an adjustment to the elevation information is necessary for constructing the DEM of special artificial terrain; and (3) the DEM correction method proposed in this paper to find the correct catchment path can ensure that the processed DEM can accurately simulate the surface catchment process, and the correction of the elevation of the road DEM is also controlled within a small range without affecting the elevation accuracy of the regional DEM. This study has reference value for implementing projects such as urban terrain expression in the construction of 3D China.



Citation: Zhao, M.; Zhao, N. Method for the Construction of Urban Road Digital Elevation Models Integrated with Semantic Information. *Appl. Sci.* **2023**, *13*, 4210. <https://doi.org/10.3390/app13074210>

Academic Editor: Jianbo Gao

Received: 28 February 2023

Revised: 20 March 2023

Accepted: 24 March 2023

Published: 26 March 2023

Keywords: digital elevation model; surface modeling; road; morphological constraints

Copyright: © 2023 by the authors. Licensee MDPI, Basel, Switzerland. This article is an open access article distributed under the terms and conditions of the Creative Commons Attribution (CC BY) license (<https://creativecommons.org/licenses/by/4.0/>).

1. Introduction

The Ministry of Natural Resources of the People's Republic of China issued the 'Notice on Comprehensively Promoting the Construction of Realistic 3D China' in February 2022 (http://gi.mnr.gov.cn/202202/t20220225_2729401.html (accessed on 24 February 2022)) (hereafter referred to as the 'Notice'). This notice takes terrain-level 3D construction as the primary task of the real 3D China construction. The specific tasks include completing 10 m and 5 m grids at the national level and completing the construction of the digital elevation model (DEM), DSM, and other data resources of the 2 m grid at the local level.

As the key foundation of the real 3D China, the precise expression of terrain plays a key role in supporting the city-level and component-level real 3D construction specified in the Notice. With the continuous development of the social economy and the continuous transformation of human activities, the earth's surface has gradually evolved into a mixed natural and artificial terrain with multiple landforms. In this context, making full use of multisource and multiscale surface observation data to achieve accurate simulation and expression of the natural and artificial mixed terrain has become the basic task of real 3D China construction, as well as a popular topic in geography, surveying, mapping, and other related fields.

In the process of expression and modeling of mixed natural and artificial terrain, road is a key element. Especially in urban areas, roads are the skeletal elements of urban terrain expression [1]. Therefore, the accurate construction of the road DEM becomes the key goal in the construction of mixed natural and artificial terrain DEM. As a typical artificial terrain, the road has the characteristics of a clear boundary and a smooth surface; therefore, the construction of the road DEM involves two basic processes, namely, road boundary information extraction and road surface DEM interpolation. The extraction of road boundary information can be attributed to feature extraction technology based on multisource multiscale images, Lidar, and other data. This topic is widely discussed in the fields of remote sensing and photogrammetry, as well as in other fields, and has achieved fruitful research results, such as extracting the building base range of urban areas based on different DEM data [2], combining image data with the DEM [3] and LIDAR data [4], using image and LIDAR point cloud and other data to extract road boundary information in urban areas [5–7], extracting water network boundary information in urban areas based on image data [8], extracting bare land area boundaries in urban areas [9], etc. Using high-definition image data to detect changes in urban areas, as well as to extract surface land use type classification, can also produce rich terrain entity boundary information [10,11]. In recent years, the depth learning method has also been introduced into the field of image processing, and relevant scholars have achieved good results by applying this method in the fine classification of the surface cover [12–16].

In terms of road DEM construction, Gao [17] discussed this problem early on, and his research also recognized the difference between the road and its background area; thus, he proposed that the road boundary be extracted first before using the elevation point information available on the road surface to construct the road DEM in the form of irregular triangulation. He also considered basic issues such as road surface elevation information inspection, available elevation point screening, etc. However, the mature TIN construction method is used for DEM development in this study. Because the irregular triangular network and the regular shape of the road surface are contradictory, the constructed road DEM does not have a perfect shape expression. Wang et al. [18] discussed the DEM modeling method of artificial terrain, such as roads, in cities from the perspective of surface water catchment analysis. This research is based on vehicle-mounted laser point cloud data. On the basis of urban feature classification data, the original point cloud data have been carefully filtered and manually edited. At the same time, the DEM of different terrain elements has been edited and processed according to the water catchment function, and, consequently, its modeling results are well expressed. However, it does not assign enough importance to the morphological expression of the road surface. Polat et al. [16] took InSAR as the main data source to discuss the construction of the road DEM in different landforms. The study focused on the elevation error of the road DEM, and did not consider the morphological characteristics of road pavement.

As mentioned above, although their types are diverse, roads are a typical artificial terrain [19], and the shapes of different roads have common characteristics. At this time, semantic information should be integrated into the modeling process, and the road DEM construction method should be designed to realize the effective expression of common characteristics of roads. Based on this approach, this study's research team first proposed a road DEM modeling method with the road boundary line as the morphological constraint.

The main idea was to first use modeling elevation information to calculate the elevation value of the nodes on the sideline of the road, and then to obtain the densified points on the road surface by generating vertical lines between the corresponding nodes of the two road sidelines. Finally, the road DEM would be generated by interpolating the densified road elevation points [20–22]. The above research uses mainly large-scale DLG data. Subsequently, our team improved the aforementioned road DEM modeling method for dense point cloud data and achieved good results [23]. However, there are still deficiencies in the above studies, which are reflected in two main aspects. First, the above studies simplified the road into horizontal and vertical undulating banded artificial ground objects, which simplifies the road DEM modeling process, but results in great differences from the actual road shape. Second, the constructed road DEM has a good visualization effect, but it does not consider the water catchment process on the road surface; as a result, its usability is poor, and it cannot effectively facilitate research on issues such as urban surface water catchment simulation.

Based on the above analysis, this study intends to further improve the road DEM construction method on the basis of existing research. The main work involves the following three aspects. First, the road sideline and the road centerline are taken as the road macro-morphological constraint line, and the upwards and horizontal undulation characteristics of the road extension are considered. Second, form constraint equations are constructed in the transverse and longitudinal directions of the road to ensure a smooth road surface. Third, with the intention of correctly simulating the surface water catchment process, a DEM elevation correction algorithm is designed so that the processed DEM can correctly simulate the road surface water catchment process.

2. Materials and Methods

2.1. Study Area and Data

Unmanned aerial vehicles (UAVs) are widely used in the surveying and mapping industry due to their portability, flexibility, and low cost. In this paper, a university in Anhui Province and its surrounding areas were selected as the study area. The Dajiang M300RTK UAV and a matching five-lens tilt aerial camera were used for data acquisition. The planned route type was a S-type route, the altitude setting was 96 m, the course overlap was 80%, the side overlap was 70%, and the resolution of the captured image was 1.5 cm. The aerial flight operation was carried out in the survey area with the parameters described above. The UAV flew for 30 min, and the number of images in five directions was 4870, corresponding to one POS file. In addition, control points were arranged at intervals of approximately 200 m in the survey area, and some points were characteristic features in the campus. A total of 20 control points were collected. After the flight was completed, ContextCapture software was used to process the data and obtain the point cloud data; then, SCOP++ software (V5.6) was used to generate the 0.2 m resolution DEM as the reference DEM data for this study. Figure 1 shows an image of the final mosaic processing in the study area.

2.2. Data Reprocessing

For the road DEM construction proposed in this study, we first obtained the road area and then extracted the sideline and centerline of the road. Therefore, the data pre-processing applied in this paper was based on feature extraction of UAV image data. Mask R-CNN is an instance segmentation algorithm proposed by Ren et al. [24] in 2017. Instance segmentation involves recognizing target contours at the pixel level. It can not only recognize different classes, but also mark multiple different objects in the same class of objects separately. Additionally, Mask R-CNN can simultaneously perform target detection and instance segmentation in a network framework [25]. Mask R-CNN uses a residual network (ResNet) to extract features, and combines it with feature pyramid network (FPN) to improve the ability to detect small targets [26]. In this paper, ResNet-50 combined with FPN is used as the backbone network to extract road boundary features.

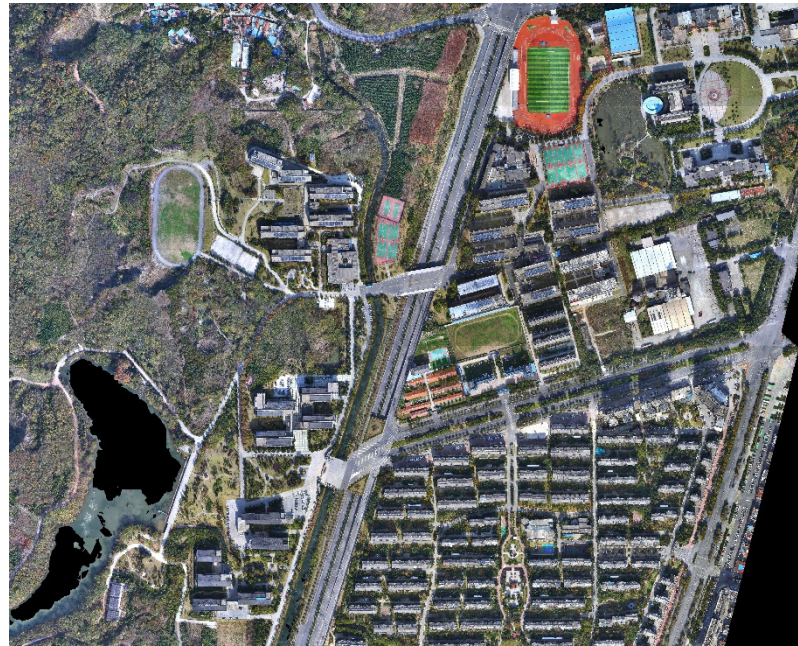


Figure 1. Image map of the study area.

Given the strong dependence of the training of the deep learning model on the number of training samples, and taking into account factors such as hardware conditions and personal capabilities, this experiment used a GPU of RTX-2060 SUPER under a Windows environment. We selected a total number of 270 samples, of which 30% of the data was designated as verification data, and the default step size was set to export the image capture of training samples. The learning rate when training all layers was 0.0001, with each maximum epoch representing the number of times that the data set would pass forwards and backwards through the neural network. It was set to 40 in the training network, and the batch size was the number of training samples to be processed at one time for training. For this experiment, we finally set the number to 8 for the training. The backbone network is set to specify the preconfigured neural network to be used as the framework for training the new model. For this experiment, ResNet-50 was selected. ResNet-50, a preconfigured model, was the residual network trained on the ImageNet dataset, which contains more than one million images and has a depth of fifty layers. The local segmentation results are shown in Figure 2.

Due to the influence of well covers, trees, vehicles, and other ground objects, boundary information derived from the terrain classification results had certain disadvantages: the shape of the segmentation edge was not accurate enough, and there were many line segment nodes. Therefore, for the terrain boundary, the point removal algorithm was used to eliminate redundant node information in the boundary line, and then the incorrect boundary information was manually modified.

2.3. Road DEM Construction Method

As a typical artificial terrain, roads have not only their own special surface morphology, but also an obvious boundary with other terrain, that is, the road boundary line. Therefore, to accurately construct the road DEM, we must begin with two tasks. The first is to determine the skeleton line of the road, that is, to determine the basic undulation characteristics of the road in the extension direction. At the early stage of research, the road is regarded as undulating in its extension direction, while in the horizontal artificial terrain, the skeleton line of the road encompasses its two sidelines. However, in reality, the road is not horizontal in the horizontal direction, but slightly bulged in the middle then lowered at both sides, especially the road with middle green belt, where this is more obvious. Thus, the road centerline is also considered a part of the road skeleton line in this study. After

determining the road skeleton line, the second part of the work was to ensure the local shape characteristics of the road surface. As mentioned above, the road surface undulated in both the road extension direction and the transverse direction. However, as the road was a type of artificial terrain with clear functions, the undulating slope in any direction was relatively small and the surface was very smooth. Therefore, the corresponding local shape control method should be designed considering these characteristics.

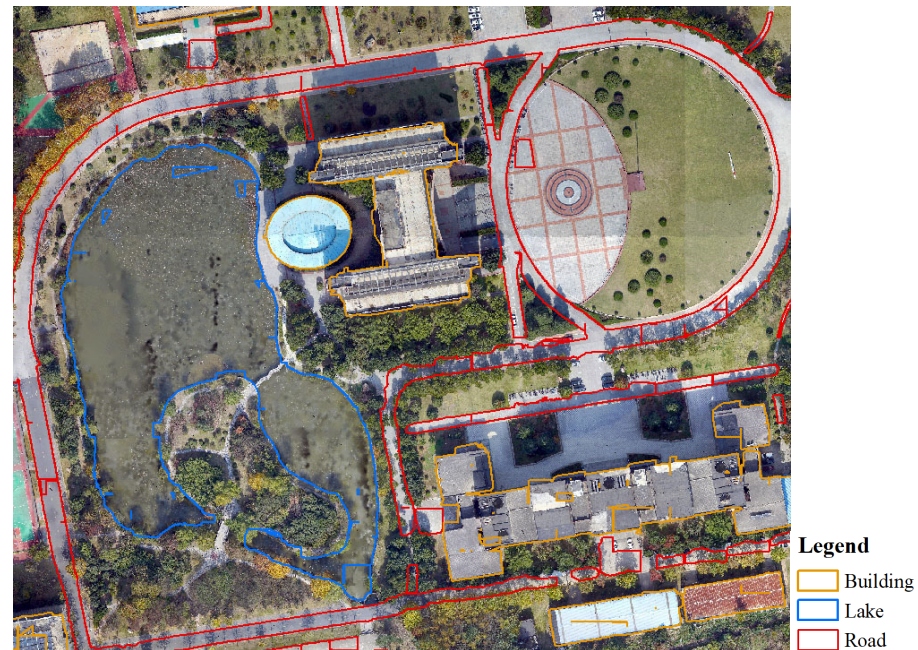


Figure 2. Split local results.

Given the above analysis, the road DEM construction method designed in this study consisted of two parts. The first part entailed the elevation assignment of the road skeleton line. The nodes were inserted into the two road sidelines and the road centerline according to a certain step length, and the initial elevation value of the relevant nodes was assigned with the Lidar point cloud as the elevation information source. Then, the node elevation value was dynamically adjusted considering the longitudinal undulation characteristics of the road. The second part involved constructing a local surface morphological constraint equation for the road to ensure that the road surface exemplified basic characteristics, such as smoothness. In addition, considering the morphological difference between the road and its adjacent terrain, after constructing the road DEM, it was necessary to consider the integration of the road DEM and other terrain DEM. Therefore, the above three tasks constitute the key methodologies of this study, which will be detailed in this section.

2.3.1. Determination of Elevation Information of Road Skeleton Line

The sidelines and road centerlines of the two roads were the control lines of the road's macroundulation shape. After the elevation of the sidelines and the centerlines was determined, the road interior could be interpolated according to road surface morphology characteristics. Therefore, the elevation calculation of the sidelines and the centerlines became the primary task of the road DEM construction. Due to the high density of LIDAR elevation points and high elevation accuracy, the calculation of elevation information on the sidelines and centerlines could be directly interpolated from LIDAR points near them, in theory. However, the shape characteristics of the road should be considered in this study. Therefore, while ensuring elevation accuracy, the elevation information of sidelines and centerlines should be further adjusted to avoid local elevation point oscillation. Based on the above ideas, the implementation process for determining the elevation information of the sideline and centerline of the road was as follows:

- (1) Read in the sideline and centerline of the road, take the grid size of the road DEM to be constructed as the step size, and insert nodes on the sideline and centerline of the road (Figure 3(1));
- (2) For the road sideline, start from the first node, take the node as the center of the circle, take the DEM grid size of the road as the radius to draw the semicircle in the road surface (Figure 3(2)), count the average elevation value of Lidar points falling into the semicircle, and assign it to the center node as the initial elevation value;
- (3) For the road centerline, start from the first node, take the node as the center of the circle, draw the circle in the road surface with the DEM grid size of the road as the radius (Figure 3(3)), count the average elevation value of Lidar points falling into the circle, and assign it to the center node as the initial elevation value;
- (4) Select a road sideline and further adjust the elevation value of the nodes on the sideline, as follows:
 - ① First, mark the first and last two points (A and B) of the sideline as noneditable, and then calculate the distance from the remaining middle nodes to the line AB. After calculation, select the corresponding node (C) with the largest distance, and mark point C as noneditable (Figures 3 and 4);
 - ② Determine a distance threshold parameter and calculate the lengths of section AC and section CB. If the length of a section is greater than the distance threshold parameter, consider the section a new road sideline and then return to step 5; if the length of the segment is less than the distance threshold parameter, smooth the remaining nodes inside the segment according to step 7;
 - ③ Starting from the second node, process each node. For the current processing node, select its left node and right node and calculate the average elevation of the three nodes together with the current processing node as the adjusted elevation value of the current processing node. If the current node has no valid elevation value, it will not be processed. Similarly, when calculating the average elevation value, if the left or right point of the current processing node has no valid elevation value, it will not be counted;
- (5) For the sideline and centerline of the other road, adjust the node elevation value according to the operation method in step (4).

2.3.2. Local Shape Control

In early DEM research, smoothness was used as a criterion for evaluating the quality of the DEM. Therefore, mathematical methods with better smoothness, such as polynomial interpolation, were also used to realize DEM elevation interpolation. Later on, with the development of earth observation technology, people began needing high-resolution DEM extraction. At this time, because it is difficult to ensure a smooth terrain at the micro scale, the smoothness of DEM results is no longer emphasized in DEM construction. However, as a kind of artificial terrain providing vehicle-driving function, smoothness is an important morphological feature of the road surface.

Among DEM construction methods, the DEM constructed by the high-accuracy surface modeling method (HASM) proposed by a research team of Chinese scholar [27–29] has good smoothness and has been successfully applied in DEM construction in different regions and at different scales. However, the HASM method is more suitable for large-scale natural terrain DEM construction, and has the best effect for terrain modeling, with multilevel undulation characteristics. For the road, although its surface smoothness is good, its undulation form is too simple, and it generally presents a quadratic parabola type, which tends to be lower on both sides with a slight bulge in the middle in the transverse direction. The undulation, for a short distance in the longitudinal direction, can also be simulated with a quadratic equation. Therefore, this study has made corresponding improvements to the original HASM method: the second derivative of the surface in the local area was

0, that is, for the local 3×3 , the central grid point in the window was analyzed, and the following equations were established:

$$f''_{p0} = \frac{f_{p3} - 2f_{p0} + f_{p2}}{2h} = 0 \tag{1}$$

$$f''_{p0} = \frac{f_{p4} - 2f_{p0} + f_{p1}}{2h} = 0 \tag{2}$$

We traversed each grid within the range of the road surface, formulated Equations (1) and (2), and then combined the corresponding equations of each point into the equation set:

$$AF = p \tag{3}$$

$$BF = q \tag{4}$$

where the precision control equation could be established from the nodes that had been assigned elevation values on the road sideline and the road centerline:

$$fp_i = k_i \tag{5}$$

All precision control equations were combined into the equation set:

$$SF = K \tag{6}$$

Referring to the calculation process of the HASM method, Equations (3), (4), and (6) were combined as a minimum extremum problem:

$$\min \left\| \begin{bmatrix} A \\ B \\ S \end{bmatrix} \cdot F - \begin{bmatrix} p \\ q \\ k \end{bmatrix} \right\|_2 \tag{7}$$

We converted the above equation into an equation set:

$$WX = V \tag{8}$$

where

$$W = A^T A + B^T B + S^T S$$

$$V = A^T p + B^T q + S^T k$$

Equation set (8) was solved to obtain the elevation value of each road grid point.

Notably, the purpose of developing Equations (1) and (2) was to establish a form constraint equation for the central grid point in the horizontal and vertical directions, but our ultimate goal was to implement the form constraint in the horizontal and vertical directions of the road. However, because the road was irregular, the horizontal and vertical directions of the road were inconsistent with the horizontal and vertical directions of the grid point. Thus, to facilitate the calculation process described above, we first converted the coordinates of points on the road. The coordinate transformation formula is

$$X = x_{left} + (l/2) + (n * l) \tag{9}$$

$$Y = y_{right} + (l/2) + (i * dis) \tag{10}$$

where (X, Y) is the transformed coordinate; (x_{left}, y_{right}) is the coordinate of the upper left corner of the outer rectangle of the road; n is the position of the n th node of the road route,

and the three road lines are sorted from top to bottom; i is the position of the current road route ($i = 0, 1, 2$); l is the grid size, that is, the step length; dis is the distance between the current road line and the first road route; $dis = \sqrt{(x_{i0} - x_{00})^2 + (y_{i0} - y_{00})^2}$, (x_{00}, y_{00}) are the coordinates of the first node of the original first road line; and (x_{i0}, y_{i0}) are the coordinates of the current road line at the first node. The transformation results are shown in Figure 4.

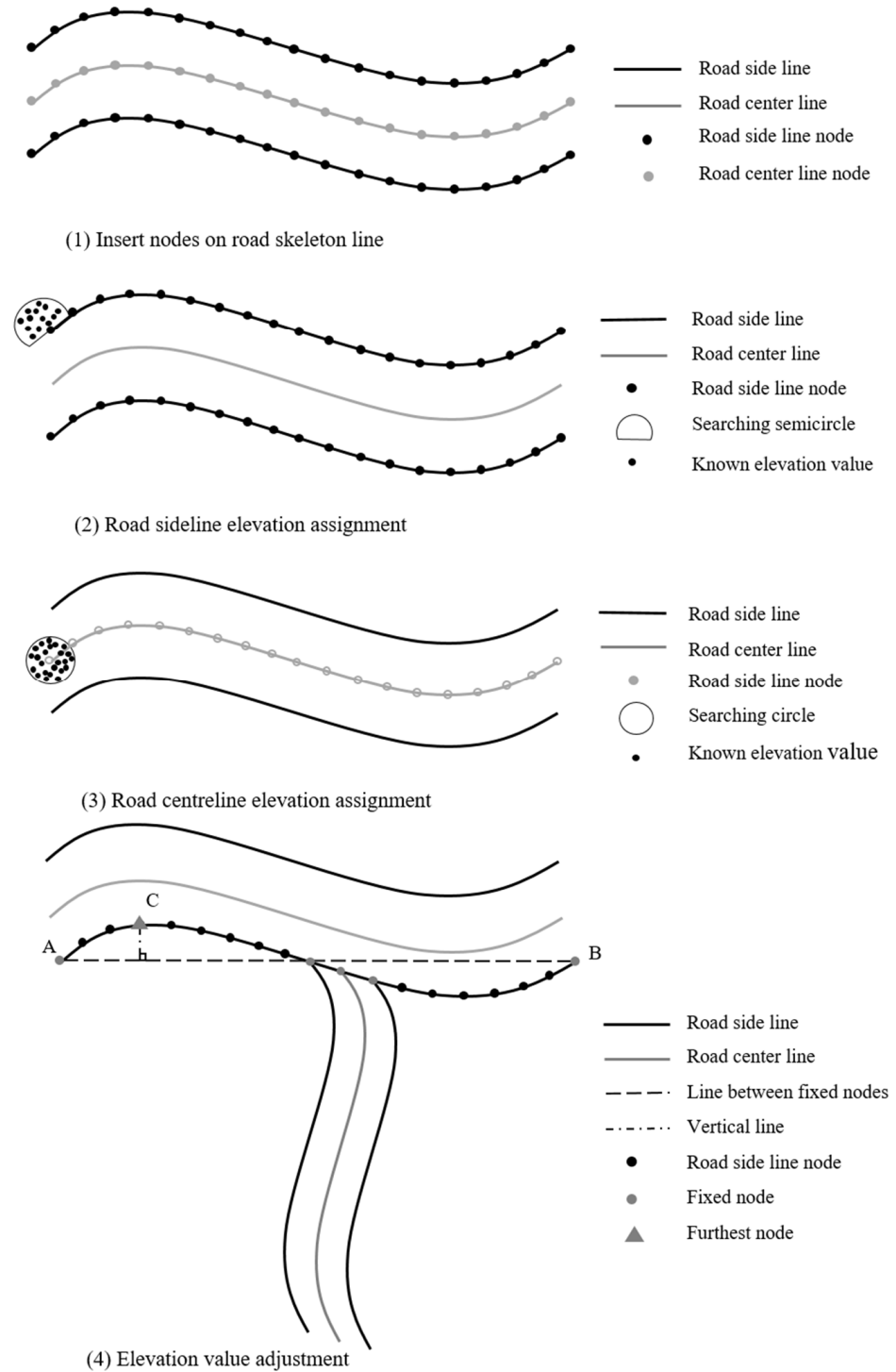


Figure 3. Elevation assignment process of the road skeleton line.

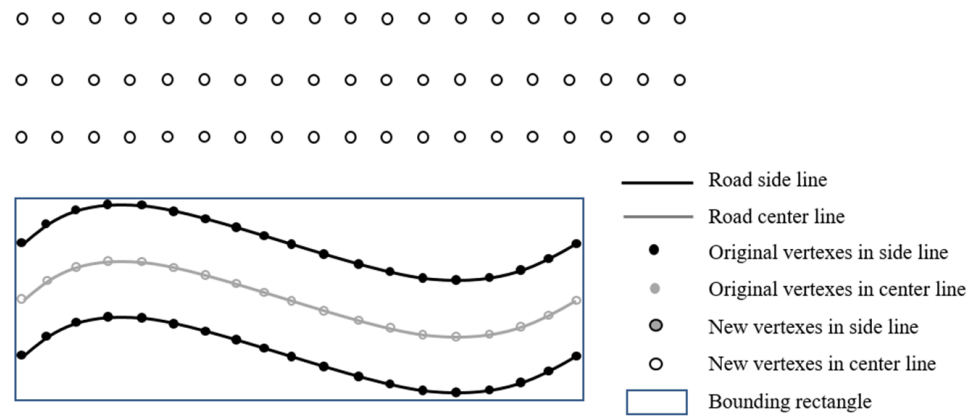


Figure 4. Coordinate transformation of road skeleton nodes.

After coordinate transformation, the nodes of the two road sidelines and the road centerline were equally spaced in the horizontal direction and corresponded to each other in the vertical direction. At this time, nodes could be inserted between the two sideline nodes and the road centerline nodes. The grid size of the road DEM to be constructed was intended to equal the step size. Then, the road surface elevation points were formed with the road sidelines and the road centerline nodes (Figure 5). At this point, the above calculation process could be used to calculate the elevation value of the road surface elevation point. After calculation, the elevation points on the road surface were obtained by the inverse coordinate transformation:

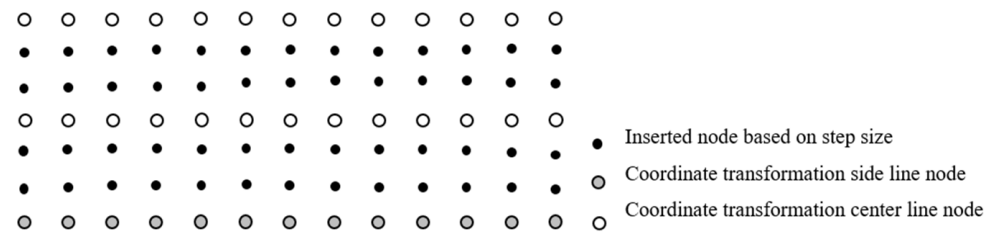


Figure 5. Road surface node composition.

For the node coordinate transformation between the first sideline and the centerline, the coordinate calculation formula was as follows:

$$X = x_{ai} + n_1 * l \tag{11}$$

$$Y = y_{ai} + n_1 * l \tag{12}$$

For the node coordinate transmission between the centerline and another sideline, the coordinate calculation formula was as follows:

$$X = x_{bi} + n_2 * l \tag{13}$$

$$Y = y_{bi} + n_2 * l \tag{14}$$

where

$$D_1 = \sqrt{(x_{bi} - x_{ai})^2} + \sqrt{(y_{bi} - y_{ai})^2}$$

$$D_2 = \sqrt{(x_{ci} - x_{bi})^2} + \sqrt{(y_{ci} - y_{bi})^2}$$

$$n_1 = 1, 2, 3, \dots, \left(\frac{D_1}{l} - 1 \right)$$

$$n_2 = 1, 2, 3, \dots, \left(\frac{D_2}{l} - 1 \right)$$

where X, Y are the coordinates after inverse transmission; l is the grid size; i is the location of the road route node; the original three road lines are sorted from top to bottom as a, b , and c ; n_1 and n_2 are the serial numbers used to mark the process point; D_1 is the distance between the nodes of route a, b at position i ; D_2 is the distance between the nodes of road line b, c at position i ; (x_{ai}, y_{ai}) are the coordinates of road line a at position i after inverse transmission; (x_{bi}, y_{bi}) are the coordinates of road line b at position i after inverse transmission; and (x_{ci}, y_{ci}) are the coordinates of road line c at position i after inverse transmission.

Because these elevation points are distributed when the grid size of the road DEM equals the step size, there is no significant difference between methods for implementing DEM interpolation at this time. In this paper, the inverse distance weighting method is used to perform road DEM interpolation.

2.3.3. DEM Optimization Considering the Water Catchment Characteristics of the Road Surface

Urban roads are the main carriers of urban traffic, and the urban drainage system is also laid mainly along the road; consequently, the road is in the main area of the urban surface catchment process. Because the urban road is relatively flat overall, the simulation of the catchment process on the road surface based on the classic surface runoff model causes serious disorder of the catchment path [30–32], which leads to failure of the catchment simulation on the road surface. This issue is also a main problem in the simulation of the urban terrain catchment process. In this study, to achieve the correct catchment function of the road surface, a DEM correction method based on the original DEM data was proposed so that the modified road DEM would be able to correctly simulate the catchment path. The main processing steps were as follows:

Step 1: Collect the water outlet in the road according to the UAV clear photographic image, read the road DEM, determine the row and column position of the water outlet in the DEM, and mark it as the water outlet grid, as shown in Figure 6(1).

Step 2: Check the grids marked as adjacent to the outlet grid, and determine the flow direction of the surrounding grids for each grid. If the current grid flows into the marked outlet grid, the grid will continue to be marked as the correct grid. Otherwise, the grid will be marked as the incorrect grid until all grid traverses are completed, as shown in Figure 6(2).

Step 3: For each grid marked incorrectly, if it flows into the grid marked as correct, mark the grid as correct. Otherwise, do not process until all incorrect grids are traversed, as shown in Figure 6(3).

Step 4: For incorrect grids that were not processed in step 3, check the surrounding grids that are marked as correct, and calculate the minimum value of the difference between the elevation of this grid and the correctly marked grid as the threshold value that must be adjusted for the current grid. At this time, the grid value is the same as a correct grid elevation value. To apply the D8 algorithm, a unit increment of 0.001 m is set to ensure that the grid value is higher than the correct grid at this time and to ensure the water flow direction, as shown in Figure 6(4).

Step 5: After the first layer of grid processing is complete, perform steps 2 to 4 for the unmarked grid until all grid processing is complete.

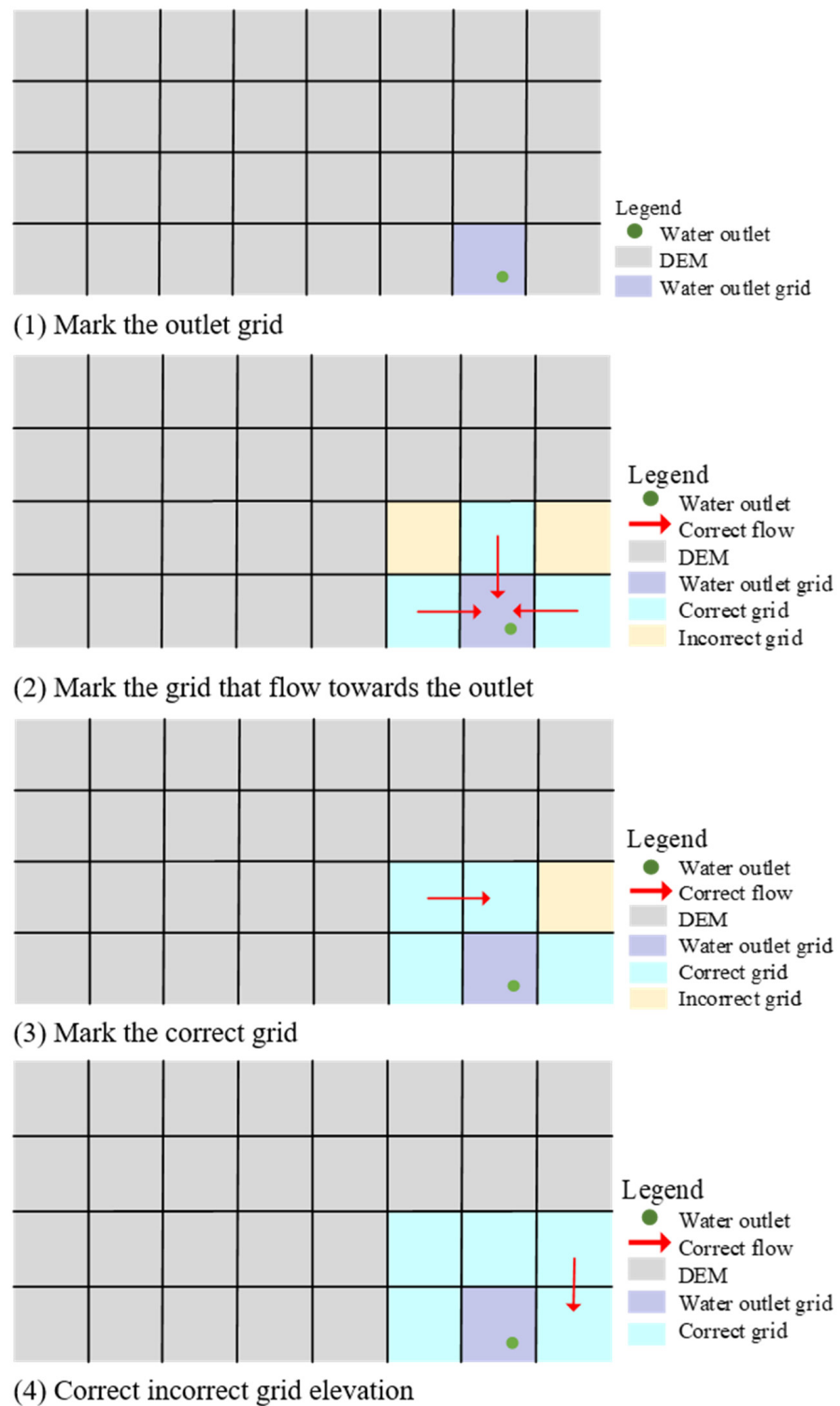


Figure 6. Road DEM correction process.

3. Results and Discussion

3.1. Road DEM Construction with Morphological Expression Priority

A typical road in the experimental area for the DEM construction experiment was selected. According to the technical process outlined in Section 2, the elevation of the road sideline and the road centerline were first assigned and adjusted. Then, the elevation

value of the road's elevation point was calculated by constructing the local shape control equation, and, finally, the road DEM was generated.

Comparing (a) and (b) in Figure 7 revealed that the elevation value of the surface of the road DEM constructed by the traditional interpolation method (IDW) in the flat terrain area was too jittery. The road should be flat; however, due to the significant fluctuation, the road's surface was rough and uneven, and the surface smoothness was poor. At the same time, the modeling method ignored the spatial element combination level of the road cross section and did not consider road shape. The road DEM constructed in this paper clearly eliminated the abnormal jitter caused by the elevation value in the traditional method, and improved the surface smoothness of the road DEM. In (c) and (d) in Figure 7, in an area with great topographic relief, the contrast between the traditional interpolation method (IDW) and the road DEM constructed by this method was not obvious because the road itself had great relief, and the elevation difference was too large. In contrast, the layered color-matching method matched colors in a certain range. When the elevation difference was too large, since its distribution color was consistent, the difference was not obvious for the road DEM in the relief area.

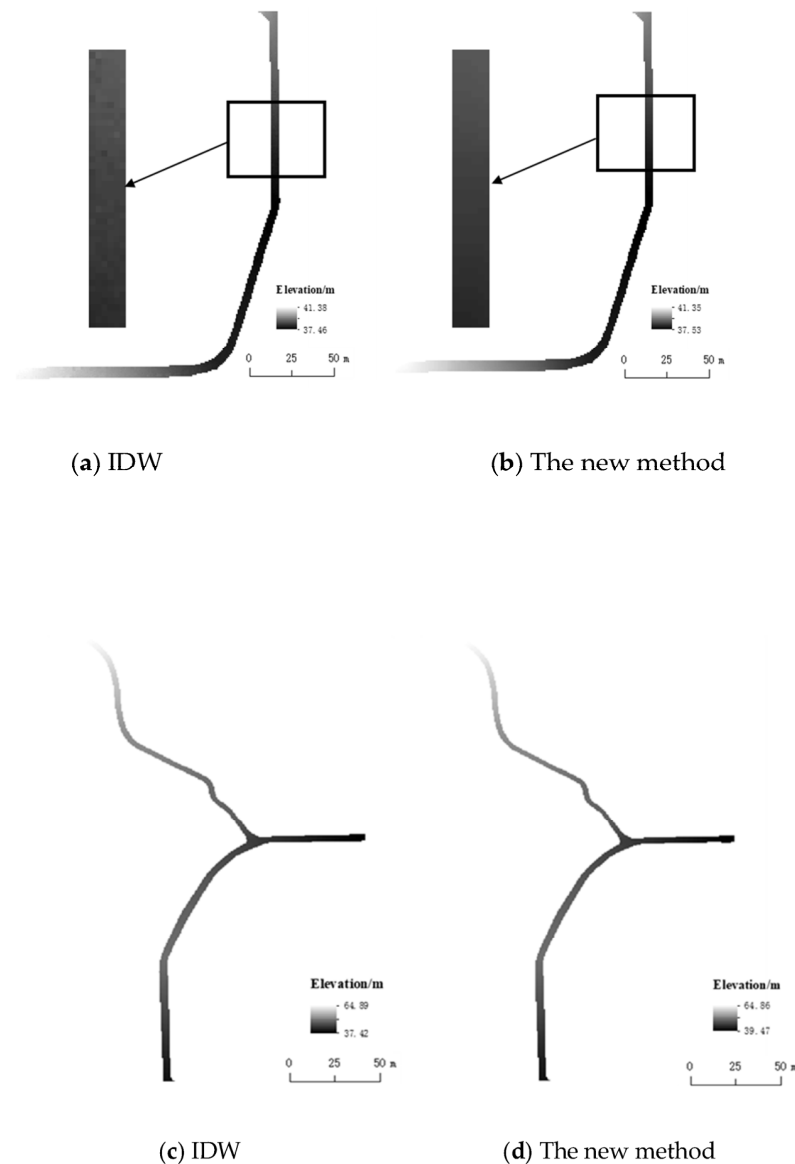


Figure 7. Road DEMs of different methods.

The morphological characteristics of the road can be intuitively expressed through the road slope analysis diagram. The slope map extracted from the results of this study and the comparison method are shown in Figure 8. The slope classification standard in this paper is based on the Code for Design of Urban Road Engineering (Ministry of Housing and Urban-Rural Development, 2012). According to the road slope map, whether in flat terrain area or undulating terrain area, an area with a large gradient extracted from the road DEM constructed by the traditional interpolation method (IDW) was relatively scattered. This was caused by excessive jitter of the elevation value of the road DEM. Moreover, it is clear that the road surface was relatively rough and uneven, resulting in a road form distortion, which did not conform to the actual terrain characteristics of the road. The road DEM built in this paper reduced excessive jitter of the road elevation value. In the flat area, the road slope was essentially within 3° . However, in the area with great topographic relief, although the slope was greater than 3° , the road slope in some areas was the same throughout the road, allowing for a smooth transition, which is consistent with the semantic characteristics of a smooth road transition.

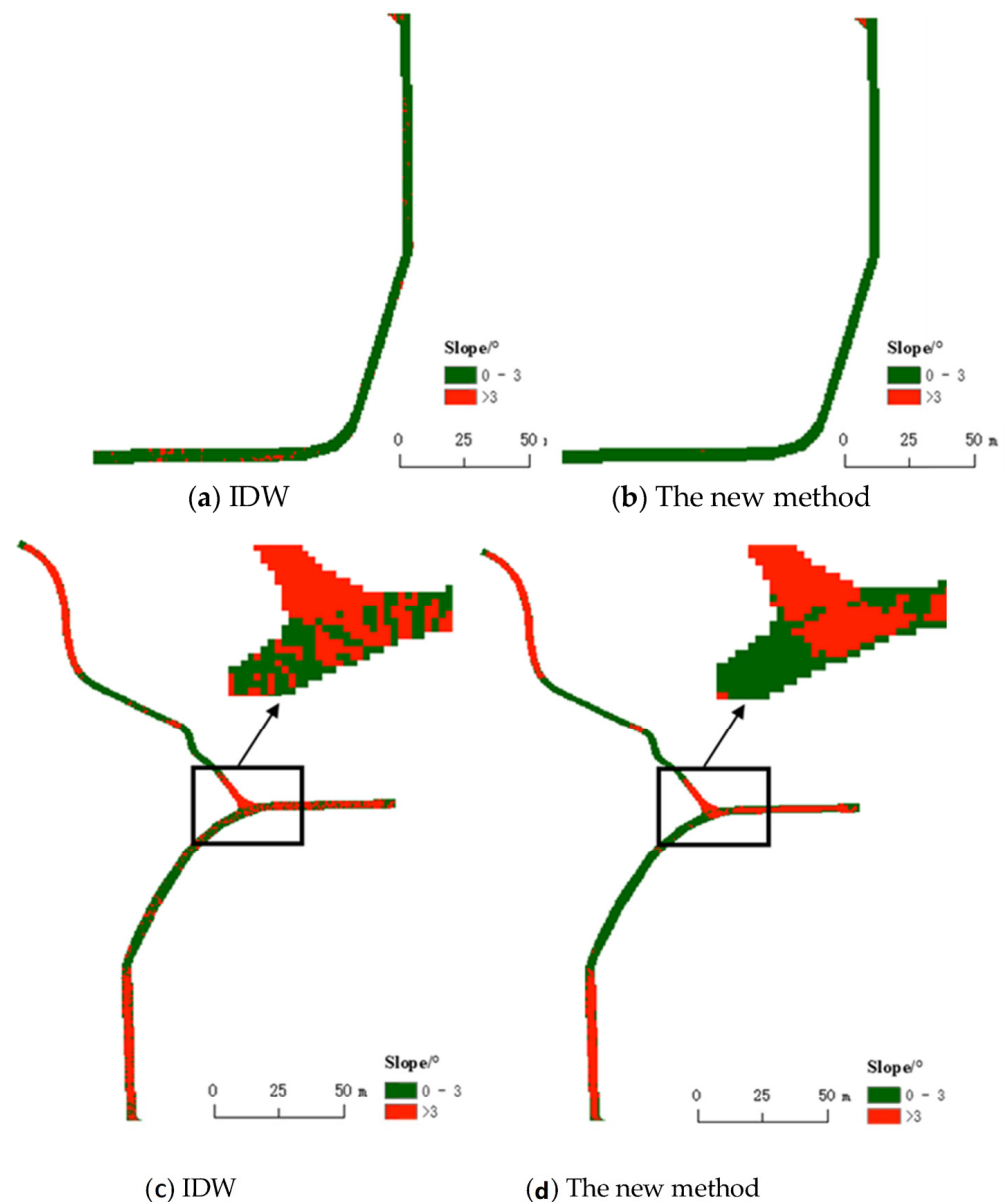


Figure 8. Road extraction slope map.

The road had the geometric and semantic characteristics of ‘horizontal singularity, vertical undulation’. The intersection was an important aspect, as it connected roads with one another. It had slightly gradual elevation fluctuation in the longitudinal direction, but showed continuity overall. Therefore, in road modeling, it is necessary to consider the smooth connection of road intersections. The intersection slope map constructed by the modeling method, such as in (c) and (d) in Figure 8, shows that the gradient distribution of the traditional interpolation method (IDW) at the intersection is uneven and the difference is too great. This indicates that the elevation difference was large on both sides of the road, making the modeling results insufficiently coherent at the intersection. The method used in this paper eliminated morphological jitter at the junction of two roads, making the intersection more consistent with the morphological characteristics of its microelevation fluctuation. However, the elevation fluctuations of the two selected sample roads were large, and the gradient at the intersection of the road was greater than 3° , which is consistent with the actual shape of the road. This result indicates that the intersection model constructed by this method conformed to the actual shape of the intersection and improved the morphological fidelity of the road modeling results.

The above road DEM and slope demonstrate that the modeling method in this paper is suitable for road modeling, and the results can conform to the morphological characteristics of the road. For quantitative analysis, several road statistics were selected for comparative analysis, and the four indicators of maximum value, minimum value, average value, and maximum elevation fluctuation were used for evaluation (Table 1). Table 1 shows that for the two road sections selected in this paper, the indexes calculated by the DEM obtained by the two methods were approximate. Statistically, the difference in each elevation index was essentially controlled at approximately 0.05 m, and the difference in the average elevation results measured by different methods was not large. However, the maximum elevation fluctuation calculated by the traditional interpolation method (IDW) for the two sections was relatively high, although the method used in this paper appropriately reduced the degree of fluctuation. Therefore, due to the characteristics of flat pavement, strong regularity of elevation change, and high accuracy and density of the modeling data, the road DEM construction method proposed in this paper resulted in no loss of elevation accuracy under the condition that the morphological accuracy was greatly improved, thus improving road smoothness and regularity.

Table 1. Statistics of road elevation index (m).

	Traditional Method (IDW)				Method Used in This Paper			
	Min.	Max.	Average	Max. Fluctuation	Min.	Max.	Average	Max. Fluctuation
Flat road	37.46	41.38	38.82	3.92	37.53	41.35	38.82	3.82
Undulating road	39.42	64.89	49.02	25.47	39.47	64.86	48.98	25.39

For the gradient of the two selected road sections (Table 2), the method in this paper significantly reduced the gradient of the road compared with the traditional interpolation method (IDW). For the flat road, the maximum gradient of the traditional interpolation method (IDW) was approximately 9° , and the gradient of the method used in this paper was controlled within 4° ; for the undulating road, the maximum gradient of the traditional interpolation method (IDW) was approximately 11° , while the gradient of the method used in this paper was controlled at approximately 9° . These results indicate that it is essential to smooth the sidelines during road construction, as this can effectively prevent outliers. Overall, the results of this method of construction not only confirmed the elevation accuracy of the DEM, but also showed that the morphological expression accuracy of the road DEM had significantly improved.

Table 2. Statistics of road gradient index (°).

	Traditional Method (IDW)			Method Used in This Paper		
	Minimum	Maximum	Average	Minimum	Maximum	Average
Flat road	0.05	7.89	1.47	0.03	4.00	0.97
Undulating road	0.01	11.61	3.24	0.05	8.95	3.08

3.2. Road DEM Construction with Functional Expression Priority

Using the road DEM correction method described in the methods section of this paper, a typical road surface with catchment function in the study area was selected to carry out DEM correction experiments. The road section was located under a hillside, and there were several outlets of underground drainage channels on one side of the road. During rainfall, water on the hillside flows to the road surface and then into the underground drainage channels through the outlets on the side of the road. To analyze and verify the construction effect of the modified road DEM more intuitively and clearly, its resolution was set to 0.2 m, and the modeling data were obtained from the road DEM and constructed based on the outlet of orthophoto image acquisition and the traditional interpolation method (IDW). The position of the water outlet in the orthophoto image is shown in Figure 9.

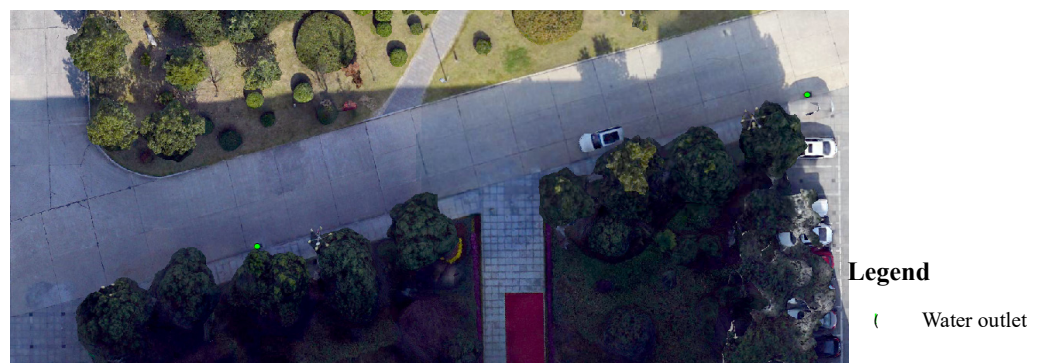


Figure 9. Distribution of water outlets in the study area.

To analyze the effect of road DEM correction, the DEM before correction (Figure 10a) was taken as the object of comparative analysis. The figure shows that the elevation difference boundary of the DEM after correction (Figure 10b) was obvious, but there was no obvious difference in elevation. The maximum elevation of the DEM after correction did not change, and the minimum elevation difference was only 1 cm, indicating that although the original road shape changed after correction, this had little impact on the elevation accuracy of the road.

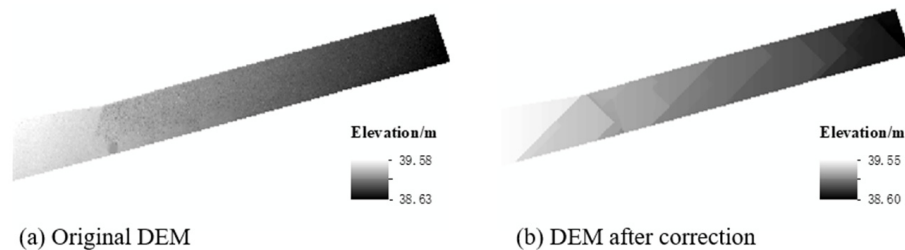


Figure 10. Correction of DEM results.

To verify the road DEM modified by the method in this paper and its functional characteristics, the DEMs constructed by the two methods were used to simulate the catchment process. The results are shown in Figure 11. The catchment path simulated by the original DEM data (Figure 11a) was disordered, with many small flows, and could

not clearly express the flow direction into the outlet. The DEM-simulated catchment path (Figure 11b), processed by the correction method proposed in this study, was able to eliminate the disordered catchment path, ensure that the catchment path pointed to the outlet in an orderly manner, and reasonably simulate the catchment process. This result indicates that the modified DEM can ensure the correct catchment function, although it has led to changes in morphology from the original DEM data.

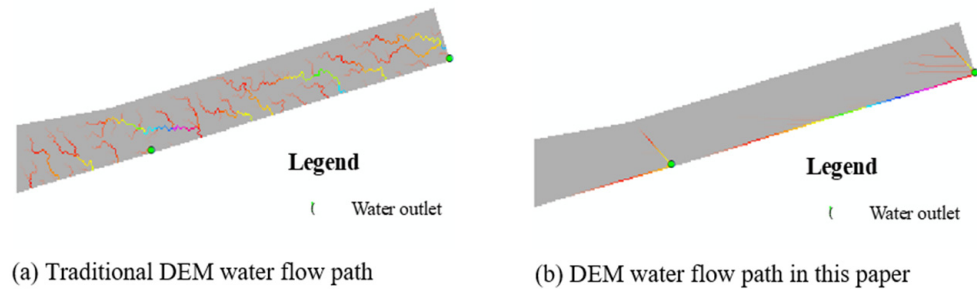


Figure 11. Comparison of water flow routes extracted by different DEMs.

Furthermore, this study calculated the difference between the modified road DEM and the original DEM data (Figure 12) and computed statistics on the distribution of grid data values in Figure 12, where the maximum value was 0.032 m and the average value was 0.009 m. The proposed DEM correction algorithm did not have an appreciable impact on the elevation accuracy of the original DEM data. For the road section examined in this study, the area where the road DEM correction algorithm changed the original road DEM greatly was on the left side of the road section. The field survey revealed that this area was slightly concave. Therefore, as shown in Figure 11a, the catchment path in this area pointed to the lower boundary of the road. In the actual precipitation process, although this area was concave, when there was too much water in the road area, the water in this area still flowed to the drain. Therefore, the function of this modified algorithm was to appropriately increase the grid unit elevation value in this area so that the modified DEM could correctly simulate the flow path.

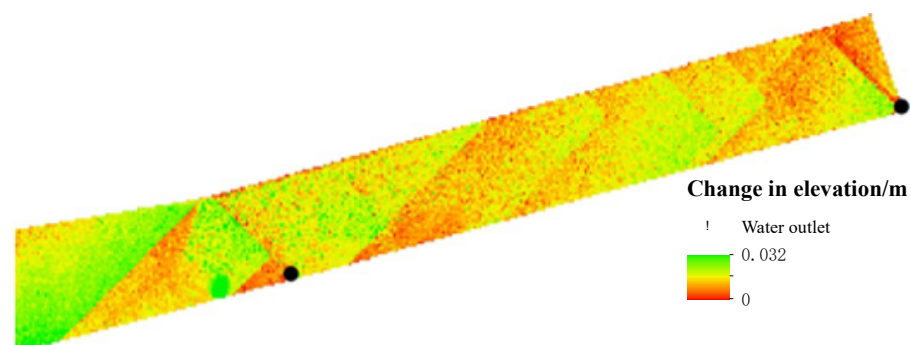


Figure 12. Difference between the modified DEM and the original DEM.

The results of this study have great application value in actual road construction and maintenance. For the new road, the simulation of the elevation of the road surface and the spatial position of the drainage outlets on both sides of the road can be carried out first to determine the best road and drainage construction plan. For the existing road, if the drainage conditions of the road are relatively poor, the current road surface can be modified according to the results of this study. This could be carried out by methods such as raising some areas or digging down some areas, so that the precipitation on the road surface can flow smoothly into the drainage outlet.

4. Conclusions

As a type of typical artificial terrain, accurate road DEM construction is an important basis for artificially mixed-terrain DEM construction. On the basis of comprehensive analysis of road semantic characteristics, this study took the high-definition image data observed by UAVs as the basic data source, designed a road DEM construction method incorporating semantic information, and developed a corresponding road DEM construction method focusing on both morphological expression priority and functional expression priority. This study selected typical experimental areas in which to carry out road DEM construction experiments. The main conclusions are as follows:

1. As an artificial surface, roads have clear functional attributes which determine the consistency of surface morphology and the elevation fluctuation of different roads in local areas. Therefore, the precise modeling of road DEM can be achieved by using the local control equation proposed in this study, which takes the sideline and centerline of the road as the macro-morphological constraints and integrates the morphological and semantic features. Slope mapping analysis demonstrated that compared with the traditional road DEM generated by the interpolation method, the road DEM shape constructed in this study is more consistent with the actual road surface.
2. The terrain modeling data used in DEM construction have high density and accuracy. At this time, the adjustment in the elevation value of the nodes on the sideline and the centerline of the road will not lead to a loss in elevation accuracy. Their purpose is to eliminate jitter in the local range of the sideline and the centerline of the road to improve the surface smoothness of the final road DEM. The statistical results of the maximum elevation, average elevation, and other parameters of the road DEM constructed by different methods in this paper indicate that the elevation difference of the road was small, and abnormal road surface jitter was eliminated.
3. For relatively flat roads, the traditional DEM generation method was unable to correctly express the surface water catchment process. However, the road surface DEM elevation correction algorithm based on the constraint of the drain proposed in this study can ensure that the backwater path of the road surface points to the drain on the side of the road, and that the runoff simulation results of the road surface are correct. At the same time, the correction algorithm had a very small impact on the elevation change in the original DEM data, resulting in an average change of less than 1 cm. The function of the surface correction algorithm is to finetune the height relationship of different locations of the road so that it can correctly simulate the surface water catchment path, but the algorithm does not affect the elevation accuracy of the road DEM.

Author Contributions: Conceptualization, M.Z. and N.Z.; methodology, N.Z.; validation, M.Z. and N.Z.; formal analysis, M.Z.; investigation, M.Z.; resources, M.Z.; data curation, N.Z.; writing—original draft preparation, M.Z. and N.Z.; writing—review and editing, M.Z. and N.Z.; visualization, N.Z.; supervision, M.Z. and N.Z.; project administration, M.Z. and N.Z.; funding acquisition, M.Z. and N.Z. All authors have read and agreed to the published version of the manuscript.

Funding: This work was supported by a grant from the Major Program of National Natural Science Foundation of China (No. 42293270), the National Program of National Natural Science Foundation of China (No. 42071374), Anhui Province Universities Outstanding Talented Person Support Project (No. gxyq2022097), Major Project of Natural Science Research of Anhui Provincial Department of Education (No. 2022AH040150), The guiding plan project of Chuzhou science and Technology Bureau (No. 2021ZD008), and the Key Project of Innovation LREIS (KPI001).

Institutional Review Board Statement: Not applicable.

Informed Consent Statement: Not applicable.

Data Availability Statement: Data are available from the corresponding author upon request by email.

Acknowledgments: We acknowledge the technical support provided by Yuanyuan Zhao.

Conflicts of Interest: The authors declare no conflict of interest.

References

1. Yang, C.; Jiang, L.; Chen, X.; Wang, C.; Zhao, M. Classification and Expression of Urban Topographic Features for DEM Construction. *J. Geo-Inf. Sci.* **2017**, *19*, 317–325.
2. Ortner, M.; Descombes, X.; Zerubia, J. A marked point process of rectangles and segments for automatic analysis of Digital Elevation Models. *IEEE Trans. Pattern Anal.* **2008**, *30*, 105–119. [[CrossRef](#)] [[PubMed](#)]
3. McNally, A.J.D.; McKenzie, S.J.P. Combining multispectral aerial imagery and digital surface models to extract urban buildings. *J. Maps* **2011**, *7*, 51–59. [[CrossRef](#)]
4. Priestnall, G.; Jaafar, J.; Duncan, A. Extracting urban features from LiDAR digital surface models. *Comput. Environ. Urban* **2000**, *24*, 65–78. [[CrossRef](#)]
5. Karathanassi, V.; Iossifidis, C.; Rokos, D. A thinning-based method for recognizing and extracting peri-urban road networks from SPOT panchromatic images. *Int. J. Remote Sens.* **1999**, *20*, 153–168. [[CrossRef](#)]
6. Youn, J.; Bethel, J.S.; Mikhail, E.M.; Lee, C.N. Extracting urban road networks from high-resolution true orthoimage and lidar. *Photogramm. Eng. Remote Sens.* **2008**, *74*, 227–237. [[CrossRef](#)]
7. Javanmardi, M.; Javanmardi, E.; Gu, Y.L.; Kamijo, S. Towards High-Definition 3D Urban Mapping: Road Feature-Based Registration of Mobile Mapping Systems and Aerial Imagery. *Remote Sens.* **2017**, *9*, 975. [[CrossRef](#)]
8. Wang, K.; Xiao, P.; Feng, X.; Wu, G.; Li, H. Extraction of urban rivers from high spatial resolution remotely sensed imagery based on filtering in the frequency domain. *J. Remote Sens.* **2013**, *17*, 269–285.
9. Palamuleni, L.G.; Ndou, N.N. Developing Remote Sensing Methodology to Distinguish Urban Built-up Areas and Bare Land in Mafikeng Town, South Africa. In Proceedings of the 2014 IEEE International Geoscience and Remote Sensing Symposium (IGARSS), Quebec City, QC, Canada, 13–18 July 2014; pp. 2205–2208.
10. Bhaskaran, S.; Paramananda, S.; Ramnarayan, M. Per-pixel and object-oriented classification methods for mapping urban features using Ikonos satellite data. *Appl. Geogr.* **2010**, *30*, 650–665. [[CrossRef](#)]
11. Chen, C.F.; Chang, L.Y. Rapid change detection of land use in urban regions with the aid of pseudo-variant features. *J. Appl. Remote Sens.* **2012**, *6*, 63574. [[CrossRef](#)]
12. Zhao, W.Z.; Du, S.H. Learning multiscale and deep representations for classifying remotely sensed imagery. *ISPRS J. Photogramm. Remote Sens.* **2016**, *113*, 155–165. [[CrossRef](#)]
13. Alshehhi, R.; Marpu, P.R.; Woon, W.L.; Dalla Mura, M. Simultaneous extraction of roads and buildings in remote sensing imagery with convolutional neural networks. *ISPRS J. Photogramm. Remote Sens.* **2017**, *130*, 139–149. [[CrossRef](#)]
14. Chen, C.C.; Jiang, F.; Yang, C.F.; Rho, S.; Shen, W.Z.; Liu, S.H.; Liu, Z.G. Hyperspectral classification based on spectral-spatial convolutional neural networks. *Eng. Appl. Artif. Intell.* **2018**, *68*, 165–171. [[CrossRef](#)]
15. Lv, X.W.; Ming, D.; Chen, Y.Y.; Wang, M. Very high resolution remote sensing image classification with SEEDS-CNN and scale effect analysis for superpixel CNN classification. *Int. J. Remote Sens.* **2019**, *40*, 506–531. [[CrossRef](#)]
16. Zhao, X.M.; Gao, L.R.; Chen, Z.C.; Zhang, B.; Liao, W.Z.; Yang, X. An Entropy and MRF Model-Based CNN for Large-Scale Landsat Image Classification. *IEEE Geosci. Remote Sens. Lett.* **2019**, *16*, 1145–1149. [[CrossRef](#)]
17. Gao, X. *Study on DEM Construction of Suburban Road Based on Large Scale Topographic Map*; Shandong University of Science and Technology: Qingdao, China, 2011.
18. Wang, Z.; Sun, Y.; Li, X. Urban DEM construction considering surface catchment analysis. *J. Geo-Inf. Sci.* **2017**, *18*, 1608–1614.
19. Sefercik, U.G.; Yastikli, N.; Dana, I. DEM Extraction in Urban Areas Using High-Resolution TerraSAR-X Imagery. *J. Indian Soc. Remote Sens.* **2014**, *42*, 279–290. [[CrossRef](#)]
20. Yang, C.C.; Zhao, M.W.; Wang, C.; Deng, K.; Jiang, L.; Xu, Y. Urban road DEM construction based on geometric and semantic characteristics. *Earth Sci. Inform.* **2020**, *13*, 1369–1382. [[CrossRef](#)]
21. Zhao, M.W.; Jiang, L.; Wang, C.; Yang, C.C.; Yang, X. On the topographic entity-oriented digital elevation model construction method for urban area land surface. *Front. Earth Sci.* **2021**, *15*, 580–594. [[CrossRef](#)]
22. Zhao, M.; Jin, Y.; Jiang, L.; Wang, C.; Yang, C.; Xu, Y. Research on DEM construction method of suburban area under multi-model coordination. *J. Geo-Inf. Sci.* **2020**, *22*, 389–398.
23. Wang, Z.; Zhao, S. Road Traffic Sign Recognition Based on Mask R-CNN. *J. Geomat.* **2022**, *47*, 119–122.
24. Ren, S.Q.; He, K.M.; Girshick, R.; Sun, J. Faster R-CNN: Towards Real-Time Object Detection with Region Proposal Networks. *IEEE Trans. Pattern Anal.* **2017**, *39*, 1137–1149. [[CrossRef](#)] [[PubMed](#)]
25. Wang, J.; Zhao, M.; Yang, C.; Fang, Y. An urban road DEM construction method based on UAV point cloud and considering morphological characteristics. *Geogr. Geoinf. Sci.* **2022**, *38*, 10–16.
26. Dollar, P.; Appel, R.; Belongie, S.; Perona, P. Fast Feature Pyramids for Object Detection. *IEEE Trans. Pattern Anal. Mach. Intell.* **2014**, *36*, 1532–1545. [[CrossRef](#)]
27. Yue, T.X. *Surface Modeling: High Accuracy and High Speed Methods*; CRC Press: Boca Raton, FL, USA, 2017.
28. Yue, T.X.; Liu, Y.; Zhao, M.W.; Du, Z.P.; Zhao, N. A fundamental theorem of Earth's surface modelling. *Environ. Earth Sci.* **2016**, *75*, 751. [[CrossRef](#)]

29. Yue, T.X.; Zhao, N.; Liu, Y.; Wang, Y.F.; Zhang, B.; Du, Z.P.; Fan, Z.M.; Shi, W.J.; Chen, C.F.; Zhao, M.W.; et al. A fundamental theorem for eco-environmental surface modelling and its applications. *Sci. China Earth Sci.* **2020**, *63*, 1092–1112. [[CrossRef](#)]
30. Saksena, S.; Merwade, V. Incorporating the effect of DEM resolution and accuracy for improved flood inundation mapping. *J. Hydrol.* **2015**, *530*, 180–194. [[CrossRef](#)]
31. Hsu, Y.C.; Prinsen, G.; Bouaziz, L.; Lin, Y.J.; Dahm, R. An Investigation of DEM Resolution Influence on Flood Inundation Simulation. *Procedia Eng.* **2016**, *154*, 826–834. [[CrossRef](#)]
32. Fereshtehpour, M.; Karamouz, M. DEM Resolution Effects on Coastal Flood Vulnerability Assessment: Deterministic and Probabilistic Approach. *Water Resour. Res.* **2018**, *54*, 4965–4982. [[CrossRef](#)]

Disclaimer/Publisher’s Note: The statements, opinions and data contained in all publications are solely those of the individual author(s) and contributor(s) and not of MDPI and/or the editor(s). MDPI and/or the editor(s) disclaim responsibility for any injury to people or property resulting from any ideas, methods, instructions or products referred to in the content.